Clay Minerals (2021), **56**, 299–305
doi:10.1180/clm.2022.11

CAMBRIDGE UNIVERSITY PRESS

Article

Measurement of apparent sintering activation energy for densification of clays

André Biava Comin[1], Alexandre Zaccaron[1]*, Vitor de Souza Nandi[1], Jordana Mariot Inocente[1], Thuani Gesser Muller[2], Alexandre Gonçalves Dal Bó[1], Adriano Michael Bernardin[1] and Michael Peterson[1,2]

[1]Post-Graduate Program on Materials Science and Engineering – PPGCEM, Universidade do Extremo Sul Catarinense, Avenida Universitária 1105, Criciúma, Santa Catarina, 88806-000, Brazil and [2]Reactors and Industrial Processes Laboratory – LabRePI, Parque Científico e Tecnológico, Rodovia Jorge Lacerda 3800, Criciúma, Santa Catarina, 88807-400, Brazil

Abstract

Clays are raw materials with properties that are necessary for the manufacture of ceramic tiles. The characteristics of clay ceramic raw materials may vary within the same mineral deposit. Clay blending promotes better use of clay reserves, thereby increasing the applicability and life cycle of raw materials. Therefore, it is important to understand the mechanisms controlling the firing of ceramic tiles. In this study, three different clays from a clay deposit were assessed and ten formulations were prepared using the mixture design method. The formulations were analysed using differential thermal and thermogravimetric analyses and dilatometric analysis. Subsequently, the most refractory and fluxing formulations were subjected to thermal tests under various heating rates, similar to the process used for the calculation of apparent sintering activation energy for the densification of clays and for pyroplasticity tests. It is suggested that a mineral deposit can be assessed based on activation energy and thermal kinetics, expanding the alternatives available to the miner through the planning of mixtures with various clays and thus reducing the energy costs of the industrial process.

Keywords: activation energy, ceramic tiles, clay, kinetics

(Received 5 June 2021; revised 12 March 2022; Accepted Manuscript online: 16 March 2022; Associate Editor: João Labrincha)

The manufactuer of ceramic tiles is evolving constantly, and current trends aim to improve the production process and technical characteristics of products. The industry is dependent on the technical characteristics of the raw materials used; therefore, there is a need to find substitutes that could reduce production costs while maintaining or improving the quality of the final product (do Livramento *et al.*, 2017).

Variability of clay properties within a single mineral deposit is very common and so exploration of mineral deposits can be inefficient. Blending of various clays therefore provides an opportunity to better use clay reserves and increase the miner-ceramist's portfolio for application to the ceramics industry (Sanfeliu & Jordán, 2009; Bordeepong *et al.*, 2012).

The thermal behaviour of clays and the phenomena caused by thermal treatment have been studied widely (Jordán *et al.*, 1999, 2020; Pardo *et al.*, 2011; Chalouati *et al.*, 2020; Semiz & Çelik, 2020). Thus, assessment of thermal behaviour in mixtures of various clays from a single mineral deposit is pivotal for industrial applications because doing so allows us to make use of all of the variations of the clay in a deposit.

During the ceramic-tile manufacturing process, firing is vital for obtaining the desired properties of the final product as thermal energy is transferred to promote a series of chemical and physical reactions such as thermal decomposition, allotropic transformation, the formation of a liquid phase and sintering (Moreno *et al.*, 2009; Cargnin *et al.*, 2011, 2015). By considering the energy changes involved during heat treatment, it is possible to obtain information regarding the reactions that occur during firing of a ceramic body (Vaughan, 1955).

The implementation of fast firing cycles has contributed significantly to the growth of the ceramic tile sector in recent decades. Products that were once fired in hour-long firing cycles are now fired in just a few minutes (Magalhães *et al.*, 2014). Another important point regarding the final properties in ceramic materials is the maximum firing temperature; currently, porcelain firing processes at temperatures of ~1160–1230°C are used (Eren *et al.*, 2017; Gültekin, 2018).

In addition, during the firing process, great caution is required to minimize defects in the end products. For example, pyroplastic deformation occurs at this stage and is influenced by stress levels in the sample. Pyroplastic deformation starts at 990°C *via* the movement of low-viscosity regions and decreases significantly at temperatures >1200°C (Rambaldi *et al.*, 2007; Frizzo *et al.*, 2020).

During firing of a ceramic body, the energy required to raise the sintering temperature and all of the energies associated with the chemical reactions resulting from the heat treatment are consumed (Jouenne, 1990). This increases production costs in processes that use thermal energy for firing (Sebastião *et al.*, 2013). In the case of ceramic pastes, these reactions are associated with the decomposition of clay, where the endothermic reaction of water being released from the structure of the clay minerals is predominant (Jouenne, 1990).

*Email: alexandrezaccaron@hotmail.com

Cite this article: Comin AB, Zaccaron A, de Souza Nandi V, Inocente JM, Muller TG, Dal Bó AG, Bernardin AM, Peterson M (2021). Measurement of apparent sintering activation energy for densification of clays. *Clay Minerals* **56**, 299–305. https://doi.org/10.1180/clm.2022.11

Ceramic materials are classified as isotropic due to the physical phenomena that occur *via* thermal expansion during their sintering (Cargnin *et al.*, 2015, 2019). Therefore, understanding their sintering kinetics helps us to determine the best processing conditions that correspond to the lowest activation energies recorded in each stage of the manufacturing process (Cargnin *et al.*, 2011; Santos *et al.*, 2016). The activation energy represents a potential barrier to the diffusion processes occurring during firing. Low activation energy values indicate easier mass transport during firing, implying rapid mass transport at low temperatures (Santos *et al.*, 2016).

In this study, three different clays from the same mineral deposit were selected and ten formulations were developed using the mixture-design method. The formulations were characterized chemically and thermally and the most refractory and fluxing formulations were defined using these values. Finally, the apparent sintering activation energy for densification was determined based on the thermal analysis and thermal kinetics results of the three clays. In addition, the most refractory and fluxing formulations were identified for each defined clay to obtain the greatest production efficiencies from an application perspective.

Experimental

Three different clays selected from the same area were used in this study. The mineralogical composition of the clays was determined using X-ray diffraction (XRD) with a Bruker D8 Advance diffractometer with Cu-*K*α radiation at 40 kV and 40 mA. All of the measurements were taken in the 2–78°2θ range at a speed of 2°θ min^{-1}. Phase quantification was conducted using the Rietveld method (Rietveld, 1969). The analysis was performed using *Match! 3* software and using the Crystallography Open Database. Ten formulations were developed using the mixture-design method (Table 1). All formulations were chemically characterized using wavelength-dispersive X-ray fluorescence (WDXRF) spectrometry with a Panalytical Axios Max system. The loss on ignition (LOI) of the samples was determined after calcination at 1000°C for 3 h. Subsequently, all formulations underwent differential thermal and thermogravimetric analyses (DTA/TGA) with a simultaneous thermal analyser (Netzsch, STA 409 EP) at 20–1075°C and at a heating rate of 10°C min^{-1} in a synthetic air atmosphere (60 cm^3 min^{-1}). Dilatometric thermal analysis of the formulations was performed using a Netzsch dilatometer (DIL 402) from room temperature to the melting point of the samples at a heating rate of 10°C min^{-1} under a synthetic air atmosphere.

Based on the dilatometric test results, the samples were characterized as more fluxing or more refractory, and the apparent sintering activation energy for densification (E_a) values of the three natural clay samples and the most fluxing and most refractory mixtures were determined. The dilatometric test was then performed again with the chosen samples by changing the heating rate to 5, 10 or 15°C min^{-1}. To determine the E_a values of the samples, isoconversional methods were used to establish the relationships between $\ln[\beta_i(d\alpha/dT)]_{\alpha,i}$ and $1/T_{\alpha,i}$ (K). The linear angular coefficient multiplied by the ideal gas constant (R) provided the E_a value for each conversion α and heating rate *i* according to Equation 1 (Friedman, 2007):

$$\ln\left[\beta_i\left(\frac{d\alpha}{dT}\right)_{\alpha,i}\right] = \ln[A_\alpha f(\alpha)] - \frac{E_a}{RT_{\alpha,i}} \quad (1)$$

Table 1. Compositions of the ten ceramic mixtures consisting of the three selected clays.

	Mixture (%)									
Clay	M.1	M.2	M.3	M.4	M.5	M.6	M.7	M.8	M.9	M.10
Clay 1	100	0	0	50.0	50.0	0	67.0	16.5	16.5	33.3
Clay 2	0	100	0	50.0	0	50.0	16.5	67.0	16.5	33.3
Clay 3	0	0	100	0	50.0	50.0	16.5	16.5	67.0	33.3

Specimens were conformed to analyse the pyroplasticity index of the compositions. First, water (7 mass%) was added to the mixtures. Then, the compositions were pressed in an electrohydraulic laboratory press (Nannetti Mignon SSN/EA) at 300 kgf cm^{-2}, forming test specimens of 4 cm diameter and 1 cm height. The samples were then dried on a stove at 100°C for 24 h.

The pyroplastic deformation test is crucial in the manufacture of porcelain tiles. The test involves a permanent deviation in the planarity of a material, which occurs at high temperatures due to gravitational force. This deviation occurs because of the large amount of liquid phase formed during firing; the lower the viscosity of a material, the greater the deformation tendency (Milak *et al.*, 2007). The method used to perform this test was described by Milak *et al.* (2007).

Results and discussion

The XRD traces obtained are shown in Fig. 1. Kaolinite, illite and quartz are present in all samples. Clay 1 contains only quartz and kaolinite, whereas illite is also present in Clays 2 and 3. The results of the quantitative analysis are shown in Table 2. The studied samples differ based on their mineralogy in terms of the relative abundances of quartz, kaolinite and illite. Clay 1 is richer in quartz, has a low kaolinite content and is free of illite, indicating greater refractoriness in the ceramic formation processes. Clays 2 and 3 have illite in their compositions. The presence of illite suggests a greater alkali and chromophore oxide ($Fe_2O_3 + TiO_2 + MnO$) content,

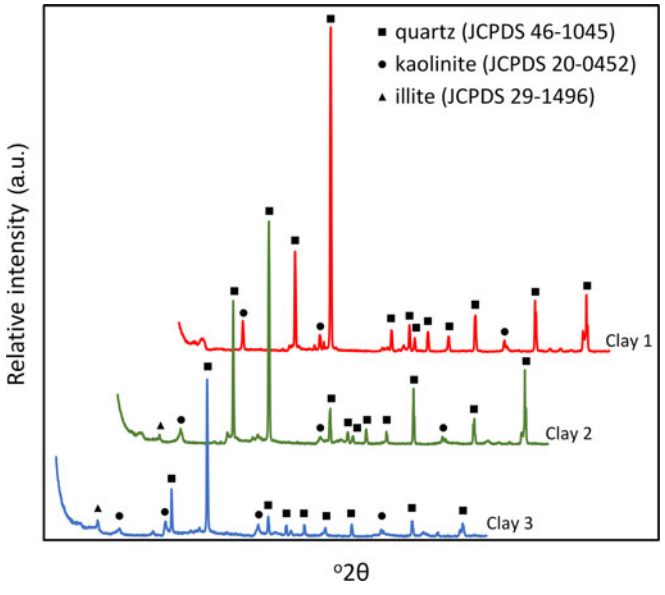

Fig. 1. X-ray traces of the clays used in this study.

https://doi.org/10.1180/clm.2022.11 Published online by Cambridge University Press

Table 2. Quantitative mineralogical compositions of the three clays.

Phase (%)	Clay 1	Clay 2	Clay 3
Quartz	82.3	61.3	48.3
Kaolinite	17.7	23.0	37.7
Illite	0	2.1	14.0

resulting in a lower melting point (Perez, 2008). Clay 3 has a greater kaolinite content, which is an important component of ceramic formulations as its conformation improves the paste workability of ceramics (Silva *et al.*, 2018).

Silica (SiO_2) and alumina (Al_2O_3) are the main chemical constituents of the ceramic mixtures (Table 3). These oxides are associated with clay minerals and quartz (Dondi *et al.*, 2001; Alcântara *et al.*, 2008). Although the high SiO_2 content favours the manufacture of type BIIb ceramic tiles (Santos *et al.*, 2016), this oxide can lead to low mechanical resistance of the sintered ceramic bodies (Seynou *et al.*, 2011).

Alkali oxides ($Na_2O + K_2O$) and alkaline-earth oxides (MgO + CaO) act as fluxes, thus facilitating the formation of a liquid phase and increasing linear shrinkage during firing (Lopez *et al.*, 2011). K_2O and MgO are abundant in mixtures containing Clay 3.

Chromophore oxides impart colouration to a ceramic body during heat treatment (Andreola *et al.*, 2013; Zanatta *et al.*, 2021). The abundance of these oxides does not exceed 3% in the mixtures. The formulations with the largest amount of Clay 3 (M.3) had the greatest chromophore oxide content. The LOI is attributed to the dehydroxylation of clay minerals and the loss of volatile materials (Vieira *et al.*, 2008; Eliche-Quesada *et al.*, 2018; Zaccaron *et al.*, 2020).

Among the secondary components, only trace P_2O_5 was identified.

Thermogravimetric analysis is useful for observing mineral reactions at higher temperatures (Comin *et al.*, 2021). Figure 2 shows mass losses corresponding to free and adsorbed water, hydroxides, kaolinite hydroxyls, CO_2 from carbonates and mullite nucleation (Mendonça *et al.*, 2012).

The mass loss due to the adsorbed water occurred at up to ~120°C (Acchar *et al.*, 2013), while at between 200 and 400°C a mass loss due to dehydroxylation of hydroxides and/or decomposition of organic matter was observed (Soares *et al.*, 2014). The mass loss due to kaolinite dehydroxylation occurred at ~500°C (Gardolinski *et al.*, 2003; Ferreira *et al.*, 2012); at ~600°C there was a mass loss associated with probable mica dehydroxylation (Menezes *et al.*, 2007).

As many ceramic minerals possess allotropic characteristics, their natural forms can be converted *via* temperature treatment into other forms with varying reversible and irreversible rearrangements, such as changes in crystalline structure and volume (Vieira & Monteiro, 2003). Figure 3 presents the DTA results for the formulations with their distinct endothermic and exothermic peaks. The formulations exhibited endothermic peaks due to the dehydroxylation of clay minerals and exothermic peaks due to the recrystallization of phases and the formation of new constituent phases.

At between 500 and 520°C, an endothermic peak was observed for kaolinite dehydroxylation (Gardolinski *et al.*, 2003; Ferreira *et al.*, 2012), and at ~560°C, a slight endothermic peak occurred, indicating the presence of quartz and its stoichiometric transformation (Galán-Arboledas *et al.*, 2017; Barreto & da Costa, 2018; Salah *et al.*, 2018). Finally, at between 960 and 980°C, an

Table 3. Chemical compositions of ceramic mixtures.

	Content (wt.%)									
Oxide	M.1	M.2	M.3	M.4	M.5	M.6	M.7	M.8	M.9	M.10
SiO_2	89.43	76.45	67.67	82.68	78.30	71.60	83.20	77.03	72.45	77.40
Al_2O_3	6.97	15.4	19.52	11.36	13.58	18.07	10.80	14.99	17.56	14.63
Fe_2O_3	0.18	0.86	1.98	0.45	0.98	1.36	0.49	0.90	1.41	0.95
CaO	–	–	–	–	–	–	–	–	–	–
K_2O	0.25	0.99	3.14	0.77	1.74	1.98	1.00	1.25	2.25	1.48
Na_2O	–	–	–	–	–	–	–	–	–	–
MgO	–	0.17	0.67	0.11	0.37	0.46	0.17	0.26	0.51	0.31
TiO_2	0.61	0.93	0.94	0.72	0.75	0.94	0.66	0.87	0.90	0.80
P_2O_5	–	0.06	0.05	–	–	0.05	–	0.05	0.05	0.05
MnO	–	–	–	–	–	–	–	–	–	–
LOI	2.47	5.11	5.96	3.67	4.02	5.34	3.46	4.47	4.68	4.21

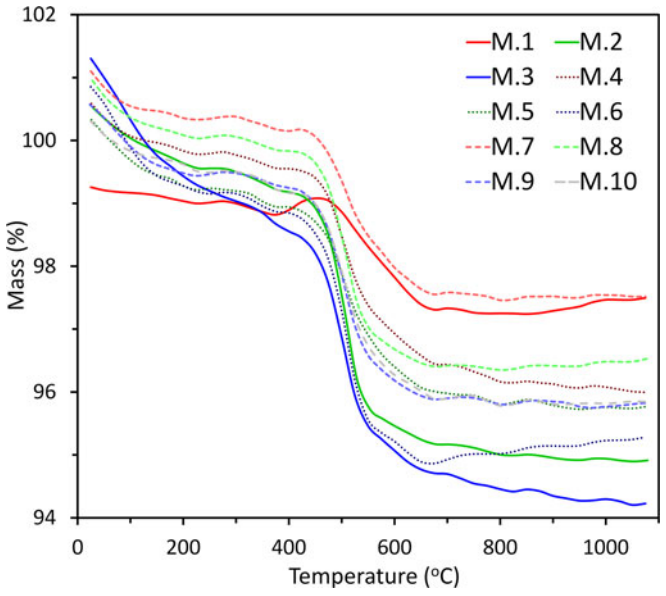

Fig. 2. TG curves of the ceramic mixtures.

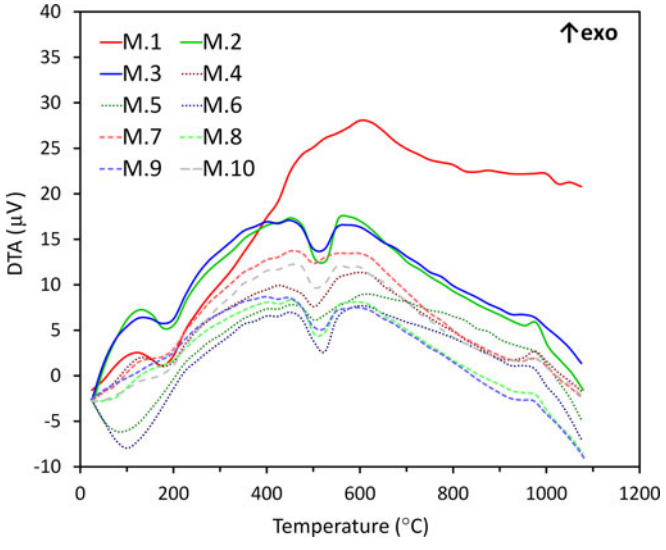

Fig. 3. DTA curves of the ceramic mixtures.

https://doi.org/10.1180/clm.2022.11 Published online by Cambridge University Press

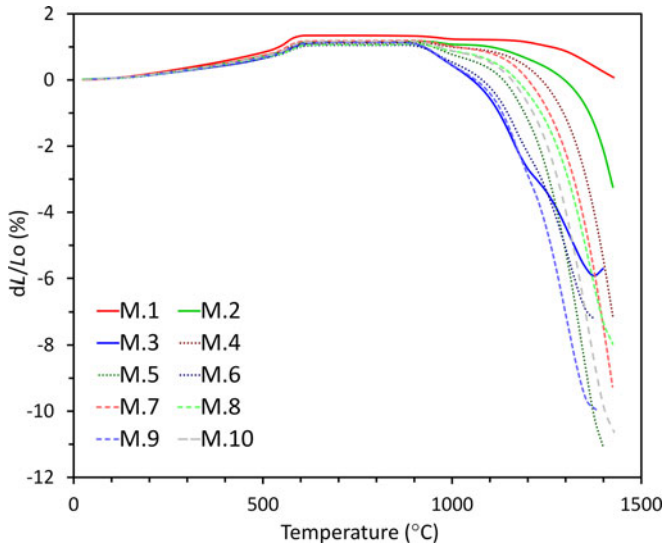

Fig. 4. Dilatometric curves of the ceramic mixtures. d*L*/*L*o = relative variation in sample length.

exothermic peak occurred due to the formation of spinel, which yielded mullite (Becker *et al.*, 2017; de Oliveira Henriques *et al.*, 2017; de Sousa *et al.*, 2017; Wang *et al.*, 2017).

Dilatometric thermal analysis (Fig. 4) initially showed the transition from α-quartz to β-quartz at ∼573°C (Schmidt-Mumm, 1991; Doppler & Bakker, 2014). At >900°C, some formulations started to retract until reaching ∼1300°C. The retraction became more accentuated at 1100°C for some formulations and continued up to 1340°C in some cases, indicating that sintering had already been initiated. The maximum sintering temperature was ∼1440°C.

The data obtained from this test indicate that the M.9 and M.4 curves represent the most fluxing and most refractory mixtures, respectively (Table 4). Moreover, intermediate fluxing and refractory curves were observed for the M.6 and M.7 mixtures, respectively. Therefore, use of Clays 1 and 2 (M.1 and M.2) increased the refractoriness of the mixtures and the addition of Clay 3 (M.3) increased the fluxing effects.

Pyroplasticity depends significantly on the ability to form liquid phases and is thus related to alkali oxides, which may form liquid phases with relatively high viscosities. Quartz in its free form (free silica) is abundant in clay, as is kaolinite, both of which increase the refractoriness of the raw material, minimizing pyroplasticity problems. In contrast, some oxides, such as Na_2O, potentially yield less viscous liquid phases, increasing the pyroplasticity index significantly (Bernardin *et al.*, 2006; Bresciani & Spinelli, 2013; Melchiades *et al.*, 2014; dos Santos Conserva *et al.*, 2017; Güngör, 2018; Frizzo *et al.*, 2020).

To analyse the pyroplasticity index (Table 5), the three clays (M.1, M.2 and M.3) and the most refractory (M.4) and most fluxing (M.9) mixtures were further analysed. Clay 2 (M.2) had a lower pyroplasticity index, primarily because of its raw density (its porosity and thus accommodation of liquid phases) and its Al_2O_3 and SiO_2 contents, facilitating the formation of structural mineral phases.

Furthermore, chemical reactions proceed rapidly when the temperature rises. This is the basis for the reactions involved in the firing of ceramic raw materials. Thus, by evaluating linear shrinkage under various heating rates at the same starting temperature (Fig. 5) and the temperatures of the various processes

Table 4. Shrinkage, start of sintering and maximum sintering temperatures of the ceramic mixtures studied.

	Temperature (°C)		
Mixture	Shrinkage	Start of sintering	Maximum sintering
M.1	910	1165	1432
M.2	1297	1338	1440
M.3	1055	1100	1315
M.4	1236	1236	1436
M.5	1135	1206	1348
M.6	921	1079	1308
M.7	1201	1201	1416
M.8	1170	1228	1365
M.9	1061	1123	1304
M.10	1158	1211	1361

Table 5. Pyroplasticity index (PI) values of the clay samples (M.1, M.2 and M.3) and of mixtures M.4 and M.9.

Sample	PI (mm^{-1})
M.1	0.199
M.2	0.064
M.3	0.118
M.4	0.148
M.9	0.167

taking place, the various energy rates required to achieve the same degree of maturation for the studied clays were determined.

With the dilatometric data generated, the respective values for densification values for each clay sample and for the most refractory and most fluxing mixtures were obtained (Table 6). This method is very sensitive, thereby highlighting the significant differences between the samples analysed. Compared to the other mixtures, the M.4 mixture exhibited the lowest E_a value (∼482 kJ) and the M.9 mixture exhibited the greatest E_a value (1492.5 kJ).

Summary and conclusion

Clays with refractory and fluxing characteristics were obtained, as assessed using thermal analyses. The mixture-design method was implemented to obtain results with the potential to expand the application of clays, such as increasing the economic viability of their industrial use.

Clay 1 (M.1) reduced the activation energy when applied in mixtures, indicating that it is a more refractory clay suitable for monoporous-type ceramics.

Clay 2 (M.2) has a low pyroplasticity index primarily because of its raw density (its porosity and thus accommodation of the liquid phases) and Al_2O_3 and SiO_2 contents, facilitating the formation of structural mineral phases. This material exhibits a high activation energy value (1399.844 kJ), demonstrating the highest activation energy value compared to the other clays (754.653 kJ for Clay 1 and 964.315 kJ for Clay 3).

Clay 3 (M.3) presented greater fluxing behaviour compared to the other materials and exhibited a greater value in terms of its pyroplasticity index because of the presence of K_2O and MgO, which potentially yield less viscous liquid phases, increasing the pyroplasticity index significantly. The thermal behaviour of this clay indicates it has an average activation energy value compared

https://doi.org/10.1180/clm.2022.11 Published online by Cambridge University Press

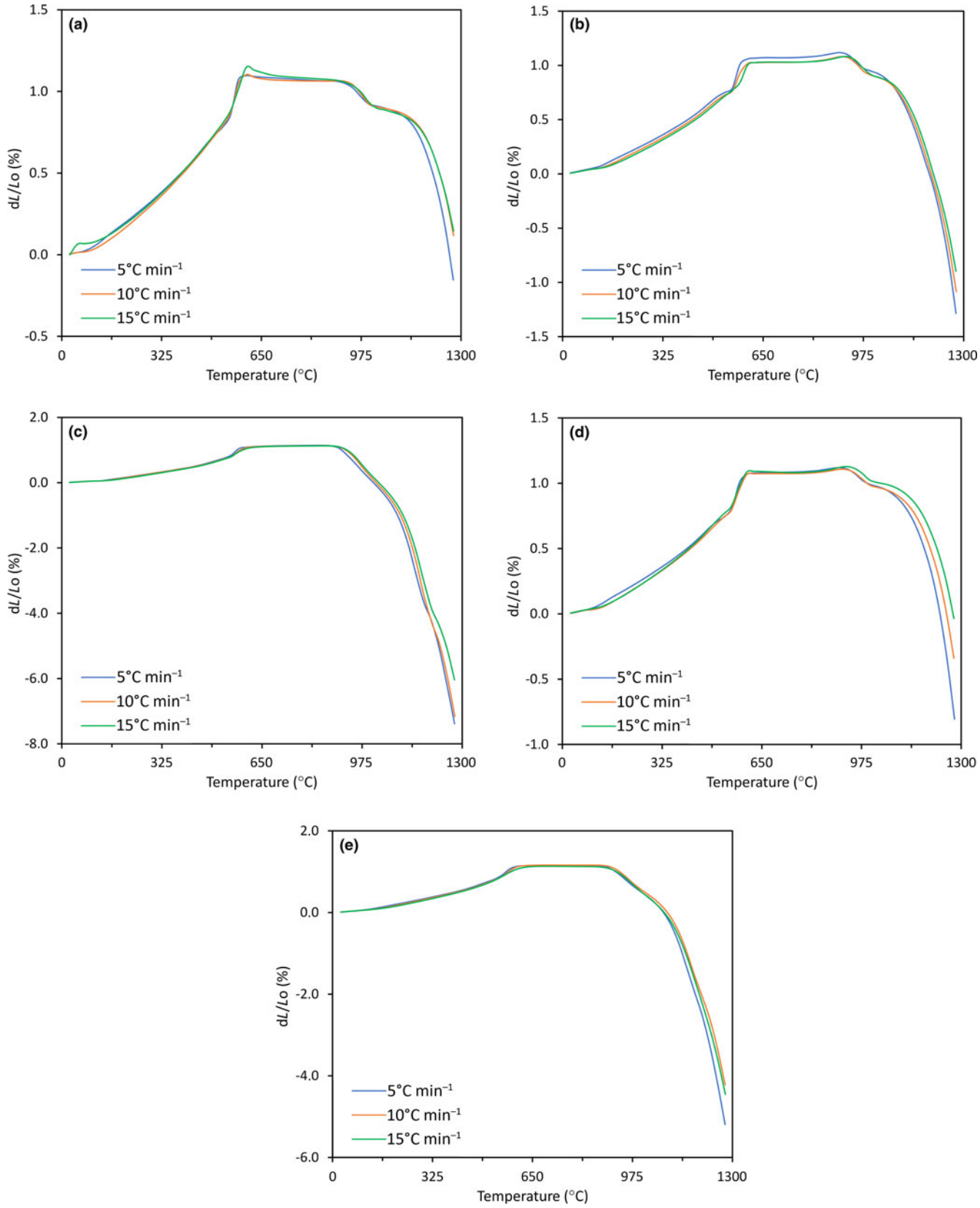

Fig. 5. Dilatometric curves of various ceramic mixtures at various heating rates: (a) M.1, (b) M.2, (c) M.3, (d) M.4 and (e) M.9. d*L*/*L*o = relative variation in sample length.

https://doi.org/10.1180/clm.2022.11 Published online by Cambridge University Press

Table 6. Apparent sintering activation energy for densification (E_a) of the clay samples (M.1, M2 and M3) and of mixtures M.4 and M.9.

Sample	E_a (kJ)
M.1	754.653
M.2	1399.844
M.3	964.315
M.4	481.721
M.9	1492.554

to the other two clays. When in a mixture composition, M.3 increases the formation of eutectic phases in pastes and can be applied in ceramic tiles that require significant vitrification, such as porcelain tiles.

Knowledge of the technological properties of materials broadens their application prospects. Hence, the use of dilatometry to characterize raw materials for application in ceramic pastes is ideal for studying closely related properties of ceramic materials, such as sintering temperature, linear shrinkage and adverse mineral reactions.

Furthermore, the influence of the kinetic evaluation of the processing data (in this case, the heating rate) of the raw materials opens new horizons for an accurate quantitative evaluation of raw materials due to considerable savings in industrial applications.

The calculation of the activation energy is important for predicting the temperature at which a desired degree of sintering can be achieved at a given heating rate. Other parameters, such as the maximum sintering temperature, may serve as a predictor in the evaluation of clay materials in industrial processes.

Author contributions. ABC: conceptualization, writing – original draft. AZ: formal analysis, writing – reviewing and editing. VdSN: methodology. JMI: validation. TGM: investigation. AGDB: formal analysis, resources. AMB: visualization, resources. MP: supervision.

Acknowledgements. The authors thank CAPES (Brazil) for the financial support of CAPES/Brazil process n. 88887.502321/2020-00 and CAPES/Brazil process n. 88887.356961/2019-00.

Conflict of interest. The authors have no conflicts of interest to declare.

References

Acchar W., Dultra E.J.V. & Segadães A.M. (2013) Untreated coffee husk ashes used as flux in ceramic tiles. *Applied Clay Science*, **75–76**, 141–147.

Alcântara A.C.S., Beltrão M.S.S., Oliveira H.A., Gimenez I.F. & Barreto L.S. (2008) Characterization of ceramic tiles prepared from two clays from Sergipe – Brazil. *Applied Clay Science*, **39**, 160–165.

Andreola F., Martín M.I., Ferrari A.M., Lancellotti I., Bondioli F., Rincón J.M. *et al.* (2013) Technological properties of glass–ceramic tiles obtained using rice husk ash as silica precursor. *Ceramics International*, **39**, 5427–5435.

Barreto I.A.R. & da Costa M.L. (2018) Viability of Belterra clay, a widespread bauxite cover in the Amazon, as a low-cost raw material for the production of red ceramics. *Applied Clay Science*, **162**, 252–260.

Becker E., Jiusti J., Minatto F.D., Delavi D.G.G., Montedo O.R.K. & de Noni Junior A. (2017) Use of mechanically-activated kaolin to replace ball clay in engobe for a ceramic tile. *Cerâmica*, **63**, 295–302.

Bernardin A.M., de Medeiros D.S. & Riella H.G. (2006) Pyroplasticity in porcelain tiles. *Materials Science and Engineering A*, **427**, 316–319.

Bordeepong S., Bhongsuwan D., Pungrassami T. & Bhongsuwan T. (2012) Mineralogy, chemical composition and ceramic properties of clay deposits in southern Thailand. *Kasetsart Journal – Natural Science*, **48**, 485–500.

Bresciani A. & Spinelli B. (2013) Deformação piroplástica em porcelanato durante a queima e variações de planaridade após a queima. *Cerâmica Industrial*, **18**, 16–20.

Cargnin M., Ulson de Souza S.M.A.G., de Souza A.A.U. & de Noni Junior A. (2011) Determinação de parâmetros cinéticos da sinterização de revestimentos cerâmicos de monoqueima do tipo BIIa. *Cerâmica*, **57**, 461–466.

Cargnin M., Kammer E.H., Ulson de Souza A.A., de Noni Junior A. & Ulson de Souza S.M.A.G. (2019) Effect of specimen geometry on kinetics of thermal decomposition of minerals in porous ceramic tiles. *International Journal of Applied Ceramic Technology*, **16**, 1098–1110.

Cargnin M., Ulson de Souza S.M.A.G., Ulson de Souza A.A. & de Noni Junior A. (2015) Modeling and simulation of the effect of the firing curve on the linear shrinkage of ceramic materials: laboratory scale and industrial scale. *Brazilian Journal of Chemical Engineering*, **32**, 433–443.

Chalouati Y., Bennour A., Mannai F. & Srasra E. (2020) Characterization, thermal behaviour and firing properties of clay materials from Cap Bon Basin, north-east Tunisia, for ceramic applications. *Clay Minerals*, **55**, 351–365.

Comin A.B., Zaccaron A., de Souza Nandi V., Inocente J.M., Muller T.G. & Peterson M. (2021) Characterization and use of clays from the Rio Bonito Formation/Paraná Basin for ceramic industry application. *International Journal of Applied Ceramic Technology*, **18**, 1814–1824.

de Oliveira Henriques J.D., Pedrassani M.W., Klitzke W., Mariano A.B., Vargas J.V.C. & Vieira R.B. (2017) Thermal treatment of clay-based ceramic membranes for microfiltration of *Acutodesmus obliquus*. *Applied Clay Science*, **150**, 217–224.

de Sousa L.L., Salomão R. & Arantes V.L. (2017) Development and characterization of porous moldable refractory structures of the alumina–mullite–quartz system. *Ceramics International*, **43**, 1362–1370.

do Livramento A., Nazário M.M., Domingos R.A., de Noni Junior A., Tassi R. & Cargnin M. (2017) Reformulação de massas para pavimentos cerâmicos fabricados pelo processo de monoqueima. *Cerâmica Industrial*, **22**, 33–40.

Dondi M., Guarini G., Ligas P., Palomba M. & Raimondo M. (2001) Chemical, mineralogical and ceramic properties of kaolinitic materials from the Tresnuraghes mining district (western Sardinia, Italy). *Applied Clay Science*, **18**, 145–155.

dos Santos Conserva L.R., Melchiades F.G., Nastri S., Boschi A.O., Dondi M., Guarini G. *et al.* (2017) Pyroplastic deformation of porcelain stoneware tiles: wet *vs.* dry processing. *Journal of the European Ceramic Society*, **37**, 333–342.

Doppler G. & Bakker R.J. (2014) The influence of the α–β phase transition of quartz on fluid inclusions during re-equilibration experiments. *Lithos,* 198–199, 14–23.

Eliche-Quesada D., Sandalio-Pérez J.A., Martínez-Martínez S., Pérez-Villarejo L. & Sánchez-Soto P.J. (2018) Investigation of use of coal fly ash in eco-friendly construction materials: fired clay bricks and silica-calcareous non fired bricks. *Ceramics International*, **44**, 4400–4412.

Eren E., Topate G. & Kurama S. (2017) The effects of sintering temperature on phase and pore evolution in porcelain tiles. *Ceramics International*, **43**, 11511–11515.

Ferreira M.M., Varajão A.F.D.C., Morales-Carrera A.M., Peralta-Sánchez M.G. & da Costa G.M. (2012) Transformações mineralógicas e cristaloquímicas decorrentes dos ensaios termais em argilas cauliníticas ferruginosas. *Cerâmica*, **58**, 105–110.

Friedman H.L. (2007) Kinetics of thermal degradation of char-forming plastics from thermogravimetry. Application to a phenolic plastic. *Journal of Polymer Science Part C: Polymer Symposia*, **6**, 183–195.

Frizzo R.G., Zaccaron A., de Souza Nandi V. & Bernardin A.M. (2020) Pyroplasticity on porcelain tiles of the albite–potassium feldspar–kaolin system: a mixture design analysis. *Journal of Building Engineering*, **31**, 101432.

Galán-Arboledas R.J., Cotes-Palomino M.T., Bueno S. & Martínez-García C. (2017) Evaluation of spent diatomite incorporation in clay based materials for lightweight bricks processing. *Construction and Building Materials*, **144**, 327–337.

Gardolinski J.E., Martins Filho H.P. & Wypych F. (2003) Comportamento térmico da caulinita hidratada. *Química Nova*, **26**, 30–35.

Gültekin E.E. (2018) The effect of heating rate and sintering temperature on the elastic modulus of porcelain tiles. *Ultrasonics*, **83**, 120–125.

Güngör F. (2018) Investigation of pyroplastic deformation of whitewares: effect of crystal phases in the 'CaO' based glassy matrix. *Ceramics International*, **44**, 13360–13366.

https://doi.org/10.1180/clm.2022.11 Published online by Cambridge University Press

Jordán M.M., Boix A., Sanfeliu T. & de la Fuente C. (1999) Firing transformations of cretaceous clays used in the manufacturing of ceramic tiles. *Applied Clay Science*, **14**, 225–234.

Jordán M.M., Montero M.A., García-Sánchez E. & Martínez-Poveda A. (2020) Firing behaviour of Tertiary, Cretaceous and Permo-Triassic clays from Castellon ceramic cluster (Spain). *Applied Clay Science*, **198**, 105804.

Jouenne C.A. (1990) *Traité de Céramiques et Matériaux Minéraux*. Septima, Paris, France, 657 pp.

Lopez S.Y.R., Rodríguez J.S. & Sueyoshi S.S. (2011) Determination of the activation energy for densification of porcelain stoneware. *Journal of Ceramic Processing Research*, **12**, 228–232.

Magalhães M., Contartesi F., dos Santos Conserva L.R., Melchiades F.G. & Boschi A.O. (2014) Efeitos do ciclo de queima sobre as temperaturas de mínima absorção de água e máxima densificação de porcelanatos. *Cerâmica Industrial*, **19**, 20–25.

Melchiades F.G., Boschi A.O., dos Santos L.R., Dondi M., Zanelli C., Paganelli M. & Mercurio V. (2014) Deformação piroplástica de porcelanatos. *Cerâmica Industrial*, **19**, 13–17.

Mendonça A.M.G.D., Cartaxo J.M., Menezes R.R., Santana L.N.L., Neves G.A. & Ferreira H.C. (2012) Expansão por umidade de revestimentos cerâmicos incorporados com residuos de granito e caulim. *Cerâmica*, **58**, 216–224.

Menezes R.R., de Almeida R.R., Santana L.N.L., Ferreira H.S., Neves G.A. & Ferreira H.C. (2007) Utilização do resíduo do beneficiamento do caulim na produção de blocos e telhas cerâmicos. *Matéria* (*Rio de Janeiro*), **12**, 226–236.

Milak A. V, Rodrigues E.P., Ricardo E.T., Tertuliano L.A., Jacinto R.P., Gastaldon R.S. *et al*. (2007) Estudo da deformação piroplástica em suportes cerâmicos obtidos com diferentes conteúdos de caulim e quartzo. *Cerâmica Industrial*, **12**, 17–21.

Moreno M.M.T., Bartolomeu D. & Lima R.H.C. (2009) Análise do comportamento de queima de argilas e formulações para revestimento cerâmico. *Cerâmica*, **55**, 286–295.

Pardo F., Meseguer S., Jordán M.M., Sanfeliu T. & González I. (2011) Firing transformations of Chilean clays for the manufacture of ceramic tile bodies. *Applied Clay Science*, **51**, 147–150.

Perez F. (2008) Fundentes: como escolher e como usar. *Cerâmica Industrial*, **13**, 31–35.

Rambaldi E., Carty W.M., Tucci A. & Esposito L. (2007) Using waste glass as a partial flux substitution and pyroplastic deformation of a porcelain stoneware tile body. *Ceramics International*, **33**, 727–733.

Rietveld H.M. (1969) A profile refinement method for nuclear and magnetic structures. *Journal of Applied Crystallography*, **2**, 65–71.

Salah I.B., Sdiri A., Jemai M.B.M. & Boughdiri M. (2018) Potential use of the lower cretaceous clay (Kef area, northwestern Tunisia) as raw material to supply ceramic industry. *Applied Clay Science*, **161**, 151–162.

Sanfeliu T. & Jordán M.M. (2009) Geological and environmental management of ceramic clay quarries: a review. *Environmental Geology*, **57**, 1613–1618.

Santos C.P., Oliveira H.A., Oliveira R.M.P.B. & Macedo Z.S. (2016) Caracterização de argilas calcárias utilizadas na produção de revestimentos cerâmicos no Estado de Sergipe – Brasil. *Cerâmica*, **62**, 147–156.

Schmidt-Mumm A. (1991) Low frequency acoustic emission from quartz upon heating from 90 to 610 °C. *Physics and Chemistry of Minerals*, **17**, 545–553.

Sebastião R.B., Fernandes P. & de Souza Nandi V. (2013) Melhoria da eficiência energética de um forno cerâmico através da troca de queimadores. *Cerâmica Industrial*, **18**, 24–30.

Semiz B. & Çelik S.B. (2020) Mineralogical and geochemical characteristics of Belevi clay deposits at Denizli, SW Turkey: industrial raw material potential. *Arabian Journal of Geosciences*, **13**, 313.

Seynou M., Millogo Y., Ouedraogo R., Traoré K. & Tirlocq J. (2011) Firing transformations and properties of tiles from a clay from Burkina Faso. *Applied Clay Science*, **51**, 499–502.

Silva A.L., Luna C.B.B., Chaves A.C. & Neves G.A. (2018) Avaliação de novos depósitos de argilas provenientes da região sul do Amapá visando aplicação na indústria cerâmica. *Cerâmica*, **64**, 69–78.

Soares R.A.L., do Nascimento R.M., Paskocimas C.A. & Castro R.J.S. (2014) Avaliação da adição de dolomita em massa de cerâmica de revestimento de queima vermelha. *Ceramica*, **60**, 516–523.

Vaughan F. (1955) Energy changes when kaolin minerals are heated. *Clay Minerals*, **2**, 265–274.

Vieira C.M.F. & Monteiro S.N. (2003) Influência da temperatura de queima na microestrutura de argilas de Campos dos Goytacazes – RJ. *Cerâmica*, **49**, 6–10.

Vieira C.M.F., Sánchez R. & Monteiro S.N. (2008) Characteristics of clays and properties of building ceramics in the state of Rio de Janeiro, Brazil. *Construction and Building Materials*, **22**, 781–787.

Wang H., Zhu M., Sun Y., Ji R., Liu L. & Wang X. (2017) Synthesis of a ceramic tile base based on high-alumina fly ash. *Construction and Building Materials*, **155**, 930–938.

Zaccaron A., de Souza Nandi V., Dal Bó M., Peterson M., Angioletto E. & Bernardin A.M. (2020) Characterization and use of clays and argillites from the south of Santa Catarina State, Brazil, for the manufacture of clay ceramics. *Clay Minerals*, **55**, 172–183.

Zanatta T., Santa R.A.A.B., Padoin N., Soares C. & Riella H.G. (2021) Eco-friendly ceramic tiles: development based on technical and market demands. *Journal of Materials Research and Technology*, **11**, 121–134.

https://doi.org/10.1180/clm.2022.11 Published online by Cambridge University Press